Nanoparticles and atoms geometro-wave potential unified and predicted properties

Z. R. Tian, Chemistry/Biochemistry, and Institute for Nanoscience/Engineering, University of Arkansas, Fayetteville, AR 72701, USA, rtian@uark.edu.

This work has introduced a geometrowave (GW) potential to linearly fit, consistently unify, and quantitatively predict and compare small particles' geometry-based properties known and new, which complements de Broglie's mass-based matter wave[1]. The "known" properties cover gold nanoparticles' (NPs') melting point and surface plasmon resonance, semiconducting NPs' optical bandgap, and main-group atoms' electronegativity (EN), ionization potential (IPs), and polarizability. The new properties include NP-surface atoms' layering (like atom-surface electrons'), self-assembled NPs' inter-bonding via sharing surface-atoms (like surface electron-shared interatomic bonding), and atom-like NPs GW-potential's periodicity like atoms electronegativity's.

For all zero-dimensional (0D), 1D-, 2D-, and 3D-particles, let's quantize their geometry-based Surface Area-to-Volume (SA/V) ratio in the unit of (length^{-1}) (see the **Extended Data Table S1**) to a geometro-wavenumber ($\tilde{\nu}_{GW}$), and their (V/SA) ratio in the unit of (length) to a geometro-wavelength (λ_{GW}), respectively. Thus, the geometro-wave potential (i.e. energy) $\mu_{GW} = hc\cdot\tilde{\nu}_{GW} = hc/\lambda_{GW}$, where the c = speed of light, h = Planck constant, and $hc \approx 1.24$ (keV·nm). The μ_{GW} is useful (see below) to prove that the pm- and nm-scales particles' long-thought "size-dependent" properties are all μ_{GW}-dependent hence geometry-quantized.

For Cd-X (X = S, Se, Te) semiconductors, for example, their 0D-NPs' optical bandgap energies (E_g) (see the **Extended Data Table S2**)[2-5] fit with their

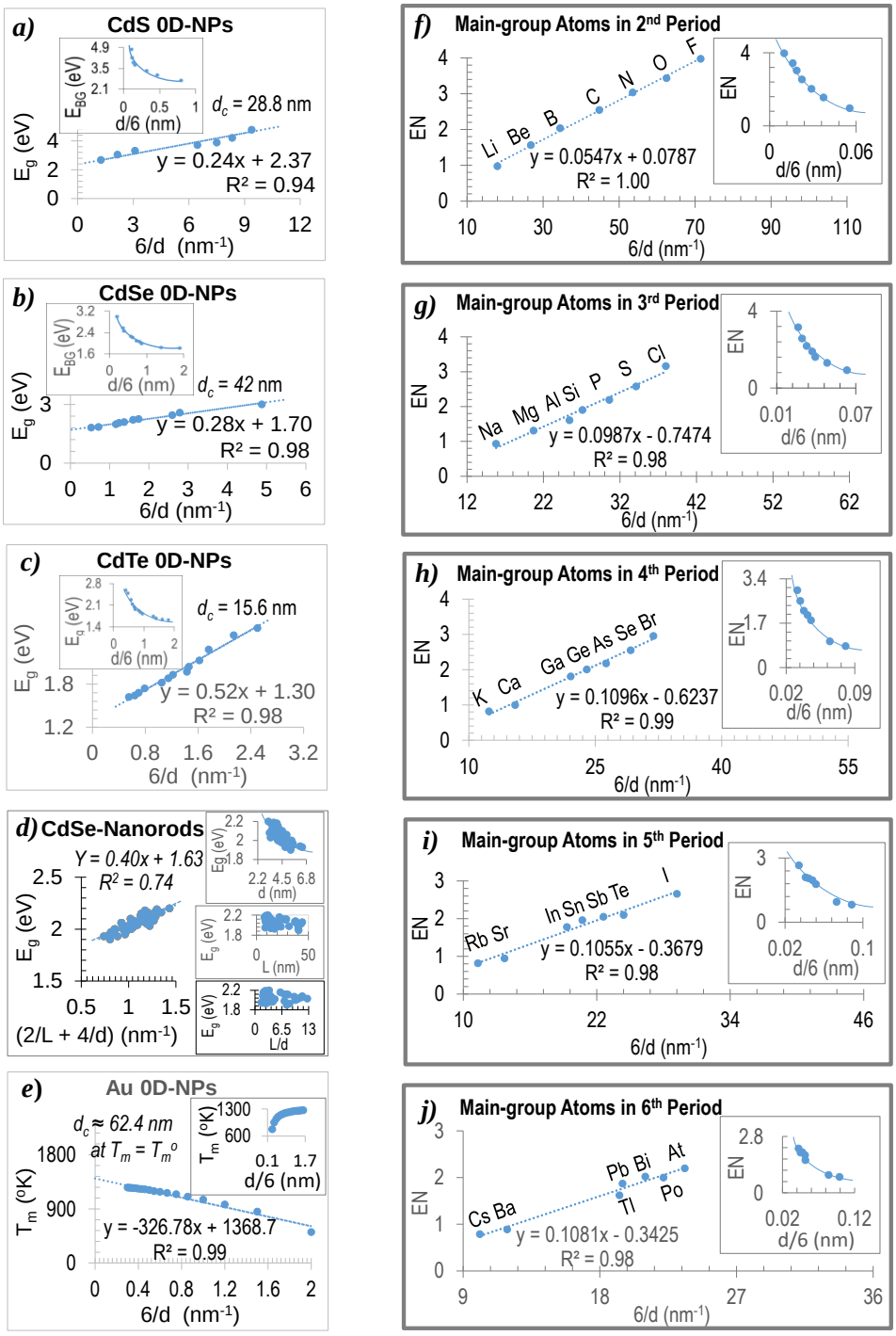

Fig. 1. Linear fits of $\tilde{\nu}_{GW}$. With the E_g of Cd-chalcogenides NPs (**a**)-(**d**), T_m of Au-0D-NPs (**e**), and EN of main-group atoms in periods (**f**)-(**j**).

$\tilde{\nu}_{GW}$ (i.e. μ_{GW}/hc) values linearly (**Figs. 1a-1c**) and with their λ_{GW} (i.e. hc/μ_{GW}) values curvedly (see the insets). From the linear equations, every intercept ≈ $E_{g(bulk)}$[6]. Further,

the trend of these linear slopes (i.e. $0.24_{(CdS-NP)} < 0.28_{(CdS-NP)} < 0.52_{(CdS-NP)}$) matches that of their $E_{g(Bulk)}$ values[6] {i.e. $2.42_{(CdS)} > 1.74_{(CdSe)} > 1.50_{(CdTe)}$ (eV)}, and that of their EN[7,8]-based bond polarities Cd–S > Cd–Se > Cd–Te. Convincingly, the scattering E_g data[9] of CdSe-nanorods fit quite linearly (**Fig. 1d**) with their $\tilde{\nu}_{GW}$ values (see the **Extended Data Table S3**), proving the generally applicable μ_{GW} selective interaction with λ_{photon}. Likewise, the Au-0D-NPs' melting points[10] (T_m) (see the **Extended Data Table S4**) fit linearly with their $\tilde{\nu}_{GW}$ values (**Fig. 1e**) and curvedly with their λ_{GW} values (the inset), showing the intercept (1368.7 ^oK) that's 2.3% off the $T_{m(bulk)}$ (1337.3 ^oK)[3]. The smaller NP's lower T_m reflects its surface atoms' lower activation energy that matches a longer electromagnetic (EM) wavelength ($\lambda_{(infrared)}$) with the NP's higher μ_{GW}.

Further, the 0D-Au-NPs' surface plasmon resonance (SPR) wavelengths (λ_{SPR})[10] and the main-group atoms' polarizability[8] (see the **Extended Data Tables S5-S6**) fit linearly with their λ_{GW} (see the **Extended Data Fig. S1**) and curvedly with their $\tilde{\nu}_{GW}$ values[11] (see two representative insets), respectively. This proves that the μ_{GW} governs the particles' surface electrons movement.

Consistently, every period of main-group atoms' Pauling EN data[7] fit linearly (**Fig. 1, f-j**) with their $\tilde{\nu}_{GW}$ and curvedly (the insets) with their λ_{GW} values[11] (see the **Extended Data Table S6**). The gap between *s*- and *p*-orbitals increases from **Fig. 1g** to **Fig. 1j** for facilitating the *d*- and *f*-blocks atoms (omitted here for clarity) support all atoms' E_{GW}-quantified and electronegativity (EN)-complemented periodicities (**Table 1**), thus-revealing the atoms' and NPs' surface-layering properties below.

First, main-group atoms' $\tilde{\nu}_{GW}$ values and first ionization potentials (or 1st IPs, in Mulliken's EN[12], see the **Extended Data Table S6**) have indeed quantified the atom-

Table 1. Periodicities of Atoms $\tilde{\nu}_{GW}$

H 0.106 **56.6** *2.20*																	**He** 0.062 **96.8**
Li 0.234 **20.6** *0.98*	**Be** 0.224 **26.8** *1.57*											**B** 0.174 **34.5** *2.04*	**C** 0.134 **44.8** *2.55*	**N** 0.112 **53.6** *3.04*	**O** 0.096 **62.5** *3.44*	**F** 0.084 **71.4** *3.98*	**Ne** 0.076 **78.9**
Na 0.380 **15.8** *0.93*	**Mg** 0.290 **20.7** *1.31*											**Al** 0.236 **25.4** *1.61*	**Si** 0.222 **27.0** *1.90*	**P** 0.196 **30.6** *2.19*	**S** 0.176 **34.1** *2.58*	**Cl** 0.158 **38.0** *3.16*	**Ar** 0.142 **42.3**
K 0.486 **12.3** *0.82*	**Ca** 0.388 **15.5** *1.00*	**Sc** 0.368 **16.3** *1.36*	**Ti** 0.352 **17.0** *1.54*	**V** 0.342 **17.5** *1.63*	**Cr** 0.332 **18.1** *1.66*	**Mn** 0.322 **18.6** *1.55*	**Fe** 0.312 **19.2** *1.83*	**Co** 0.304 **19.7** *1.88*	**Ni** 0.298 **20.1** *1.91*	**Cu** 0.290 **20.7** *1.90*	**Zn** 0.282 **21.3** *1.65*	**Ga** 0.272 **22.1** *1.81*	**Ge** 0.250 **24.0** *2.01*	**As** 0.228 **26.3** *2.18*	**Se** 0.206 **29.1** *2.55*	**Br** 0.188 **31.9** *2.96*	**Kr** 0.176 **34.1**
Rb 0.530 **11.3** *0.82*	**Sr** 0.438 **13.7** *0.95*	**Y** 0.424 **14.2** *1.22*	**Zr** 0.412 **14.7** *1.33*	**Nb** 0.396 **15.2** *1.6*	**Mo** 0.380 **15.8** *2.16*	**Tc** 0.366 **16.4** *2.10*	**Ru** 0.356 **16.9** *2.2*	**Rh** 0.346 **17.3** *2.28*	**Pd** 0.338 **17.8** *2.20*	**Ag** 0.330 **18.2** *1.93*	**Cd** 0.322 **18.6** *1.69*	**In** 0.312 **19.2** *1.78*	**Sn** 0.290 **20.7** *1.96*	**Sb** 0.266 **22.6** *2.05*	**Te** 0.246 **24.4** *2.1*	**I** 0.230 **26.1** *2.66*	**Xe** 0.216 **27.8** *2.60*
Cs 0.596 **10.1** *0.79*	**Ba** 0.506 **11.9** *0.89*	**La** 0.390 **15.4** *1.10*	**Hf** 0.416 **14.4** *1.3*	**Ta** 0.400 **15.0** *1.5*	**W** 0.386 **15.5** *1.7*	**Re** 0.376 **16.0** *1.9*	**Os** 0.370 **16.2** *2.2*	**Ir** 0.360 **16.7** *2.2*	**Pt** 0.354 **16.9** *2.2*	**Au** 0.348 **17.2** *2.4*	**Hg** 0.342 **17.5** *1.9*	**Tl** 0.312 **15.8** *1.8*	**Pb** 0.308 **19.5** *1.8*	**Bi** 0.286 **21.0** *1.9*	**Po** 0.270 **22.2** *2.0*	**At** 0.300 **20.0** *2.2*	**Rn** 0.240 **25.0**

La 0.390 **15.4** *1.10*	**Ce** 0.370 **16.2** *1.12*	**Pr** 0.370 **16.2** *1.13*	**Nd** 0.370 **16.2** *1.1*	**Pm** 0.370 **16.2**	**Sm** 0.370 **16.2** *1.17*	**Eu** 0.370 **16.2**	**Gd** 0.360 **16.7** *1.20*	**Tb** 0.350 **17.1**	**Dy** 0.350 **17.1** *1.22*	**Ho** 0.350 **17.1** *1.23*	**Er** 0.350 **17.1** *1.24*	**Tm** 0.350 **17.1** *1.25*	**Yb** 0.350 **17.1**	**Lu** 0.350 **17.1** *1.0*
Ac 0.390 **15.4** *1.1*	**Th** 0.360 **16.7** *1.3*	**Pa** 0.360 **16.7** *1.5*	**U** 0.350 **17.1** *1.7*	**Np** 0.350 **17.1** *1.3*	**Pu** 0.350 **17.1** *1.3*	**Am** 0.350 **17.1**	**Cm** 0.238 **25.2**	**Bk** 0.34 **17.6**	**Cf** 0.372 **16.1**	**Es** 0.372 **16.1**	**Fm** 0.334 **18.0**	**Md** 0.346 **17.3**	**No** 0.332 **18.1**	**Lr** 0.322 **18.1**

La
0.308
19.5
1.10

Atomic Symbol
Atomic diameter* {unit: (nm)}
$\tilde{\nu}_{GW}$ **(unit: nm^{-1})**
*Pauling's EN****

*Atomic diameters data source:
https://en.wikipedia.org/wiki/Atomic_radii_of_the_elements_(data_page) (Jan-8-2019).

**Pauling's EN data source:
Lide, D. R. *CRC Handbook of Chem. and Phys.* (CRC Press, Boca Raton, FL, 2000).

surface electrons' μ_{GW}-quantized layering in the *s*-orbital first and then *p*-orbitals before and after the half-fill (**Figs. 2a-2d**). The increasing gaps between the *s*- and *p*-orbitals (**Figs. 2b-2d**) match that in the **Figs. 1f-1j**. Further, the transition metals cations' $\tilde{\nu}_{GW}$ fits linearly with the IP[8] (see the **Extended Data Table S7** and the **Extended Data Fig. S2**), showing the d-orbitals' negligible size change before and after the half-fill.

Likewise, zooming in the **Figs. 1a-1c** has revealed the NPs' sudden (i.e. quantized) E_g drop (see the green dash-lines) as CdTe-NP's (**Fig. 2e**) < CdSe-NP's (**Fig. 2f**) < CdS-NP's (**Fig. 2g**). This supports the PbSe-0D-NPs' negligible E_g drop (see the **Extended Data Table S8** and the **Extended Data Fig. S3**), since $E_{g(\text{bulk-PbSe})} \approx 0.7$ (eV)[6] << $E_{g(\text{bulk-CdTe})}$. The E_g drop tells the NP-surface atoms' E_{GW}-quantized layering, somewhat like atom-surface electrons' (**Figs. 2a-2d**), revealing an

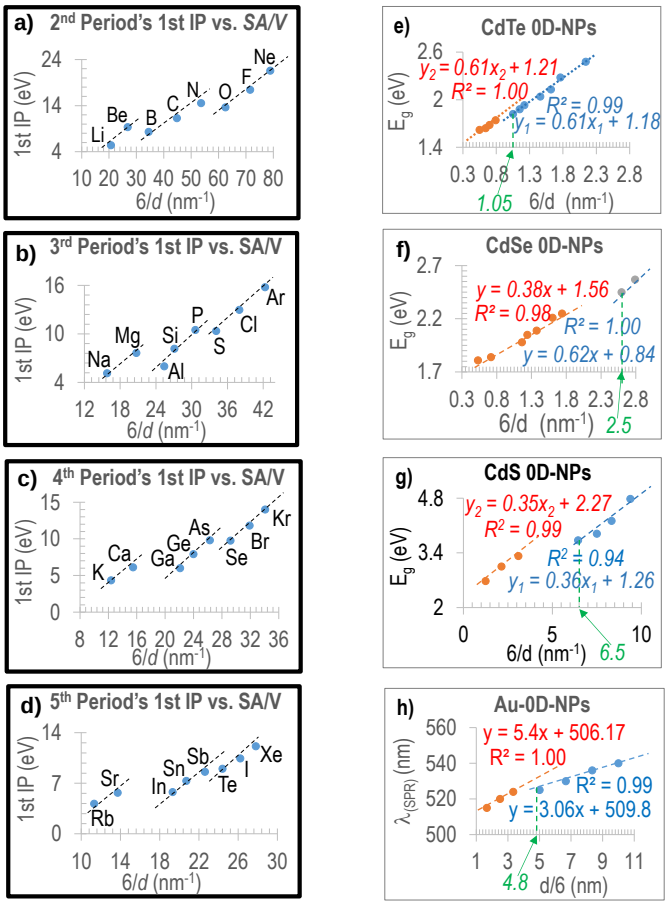

Fig. 2. Atoms' and NPs' structural layering from correlations of their $\tilde{\nu}_{GW}$. With main-group atoms 1st IP (**a**)-(**d**), with E_g for 0D-NPs of CdTe (**e**), CdSe (**f**), and CdS (**g**), and with Au-0D-NPs $\lambda_{(SPR)}$ (**h**).

*Note: The green dash-line in (**e**)-(**h**) shows the start of the sudden drop in the E_g and $\lambda_{(SPR)}$ values.*

atomistic nature[13] in smaller 0D-NPs' more blue-shifted E_g, which helps expand Bohr's atomic model (i.e. QM) to the 0D-NPs.

Further, zooming in the **Extended Data Fig. S1a** has disclosed the Au-0D-NPs' sudden drop of their (λ_{SPR}) when $\lambda_{GW} < 4.8$ (nm) (**Fig. 2h**), indicating that the Au-NPs' surface atoms do layer like the Cd-X NPs' (**Figs. 2e-2g**).

The NPs' atomistic nature (**Figs. 2e-2h**) supports the smaller NPs' stronger inter-bonding (see the **Extended Data Fig. S4**) in self-assembly[14-17] and biomineralization[18,19] via sharing their surface atoms geometrically, like smaller atoms' stronger EN-based

bonding via sharing more surface electrons electromagnetically. This proves every NP behaving like a super atom, which helps expand the particle science.

In summary, the new geometro-wave potential has been proven generally useful to complement de Broglie's matter-wave (i.e. QM), and quantitatively predict and compare and consistently unify the NPs and atoms geometry-quantized properties known and new. The new properties, including NPs' surface atoms layering, inter-NP bonding, and atoms' E_{GW}-generalized periodicity, have naturally helped derive new basics in physics, chemistry and chemical biology, which will be detailed separately.

References:

[1] de Broglie, L. The Reinterpretation of Wave Mechanics. *Foundations of Physics* **1**, 1 (1970) (https://link.springer.com/article/10.1007/BF00708650).

[2] Rossetti, R.; Nakahara, S. and Brus, L. E. Quantum size effects in the redox potentials, resonance Raman spectra, and electronic spectra of CdS crystallites in aqueous solution. *J. Chem. Phys*. **79**, 1086–1088 (1983).(https://aip.scitation.org/doi/pdf/10.1063/1.445834).

[3] Murray, C. B.; Norris and D. J.; Bawendi, M. G. Synthesis and characterization of nearly monodisperse CdE (E = Sulfur, Selenium, Tellurium) semiconductor nanocrystallites. *J. Am. Chem. Soc.* **115**, 8706–8715 (1993). (https://pubs.acs.org/doi/abs/10.1021/ja00072a025).

[4] Vossmeyer, T.; Katsikas, L.; Giersig, M.; Popovic, I. G.; Diesner, K.; Chemseddine, A.; Eychmueller, A. and Weller, H. CdS Nanoclusters: Synthesis, Characterization, Size Dependent Oscillator Strength, Temperature Shift of the Excitonic Transition Energy, and Reversible Absorbance Shift. *J. Phys. Chem.* **98**, 7665–7673 **(**1994**).** (https://pubs.acs.org/doi/abs/10.1021/j100082a044).

[5] Yu, W. W.; Qu, L.; Guo, W. and Peng, X. Experimental determination of the extinction coefficient of CdTe, CdSe, and CdS nanocrystals. *Chem. Mater*. **15** (14), 2854–2860 (2003). (https://pubs.acs.org/doi/abs/10.1021/cm034081k).

[6] Kasap, S. O. and Capper, P. *Springer handbook of electronic and photonic materials* (Springer, 2006). (https://books.google.com/books?hl=en&lr=&id=3JQ4DwAAQBAJ&oi=fnd&pg=PR5&dq=6%09Kasap,+S.+O.+and+Capper,+P.+Springer+handbook+of+electronic+and+photonic+materials+(Springer,+2006)&ots=BihP23kF_b&sig=cwuL6kbVNH2KnHvFlp-4fEi0Tuk#v=onepage&q=6%09Kasap%2C%20S.%20O.%20and%20Capper%2C%20P.%20Springer%20handbook%20of%20electronic%20and%20photonic%20materials%20(Springer%2C%202006)&f=false).

[7] Pauling, L. *The Nature of the Chemical Bond* (Cornell Univ. Press, Ithaca, 1960). (https://www.academia.edu/26073847/Pauling_L._The_nature_of_the_chemical_bond_Cornell_Univ._1960_).

[8] Lide, D. R. *CRC Handbook of Chemistry and Physics* (CRC Press, Boca Raton, FL, 2000). (http://diyhpl.us/~nmz787/mems/unorganized/CRC%20Handbook%20of%20Chemistry%20and%20Physics%2085th%20edition.pdf).

[9] Li, L.-S.; Hu, J.; Yang, W. and Alivisatos, A. P. Band gap variation of size- and shape-controlled colloidal CdSe quantum rods. *Nano Lett* **1 (7),** 349–351 (2001). (https://pubs.acs.org/doi/10.1021/nl015559r).

[10] *Gold Nanoparticles: Properties and Applications*, Sigma-Aldrich, (www.sigmaaldrich.com/technical-documents/articles/materials-science/nanomaterials/gold-nanoparticles.html).

[11] *Calculated atomic radii* (Ed. Jan-7-2019), https://en.wikipedia.org/wiki/Atomic_radii_of_the_elements_(data_page).

[12] Mulliken, R. S. A New Electroaffinity Scale; Together with Data on Valence States and on Valence Ionization Potentials and Electron Affinities. *J. Chem. Phys*. **2** (11): 782–793 (1934). (https://aip.scitation.org/doi/10.1063/1.1749394).

[13] Zunger, A. Pseudopotential theory of semiconductor quantum dots. *Phys. Stat. Sol. (b)* ***224***, 727–734 (2001). (https://doi.org/10.1002/(SICI)1521-3951(200104)224:3<727::AID-PSSB727>3.0.CO;2-9).

[14] Kresge, C. T.; Leonowicz, M. E.; Roth, W. J.; Vartuli, J. C. and Beck, J. S. Ordered mesoporous molecular sieves synthesized by a liquid-crystal template mechanism. *Nature* **359**, 710-712 (1992). (https://www.nature.com/articles/359710a0).

[15] Tian, Z. R.; Tong, W.; Wang, J. Y.; Duan, N. G.; Krishnan, V. V. and Suib, S. L. Manganese oxide mesoporous structures: mixed-valent semiconducting catalysts. *Science* **276**, 926 (1997). (https://science.sciencemag.org/content/276/5314/926).

[16] Yang, P. D.; Zhao, D.; Margolese, D. I.; Chmelka, B. F. and Stucky, G. D. Generalized syntheses of large-pore mesoporous metal oxides with semicrystalline frameworks. *Nature* **396**, 152-155 (1998). (https://www.nature.com/articles/24132).

[17] Whitesides, G. W. and Grzybowski, B. Self-assembly at all scales. *Sci*. **295**, 2418–2421 (2002). (https://science.sciencemag.org/content/295/5564/2418.full).

[18] Aizenberg, J.; Weaver, J. C.; Thanawala, M. S.; Sundar, V. C.; Morse, D. E. and Fratzl, P. Skeleton of Euplectella sp.: structural hierarchy from the nanoscale to the macroscale. *Science* **309**, 275-278 (2005). (DOI: 10.1126/science.1112255).

[19] Hua, L; Zheng, J.; Zhou, Z. R.; and Tian, Z. R. Water-Switchable Interfacial Bonding on Tooth Enamel Surface, *ACS Biomater. Sci. Eng.* **4** (7), 2364–2369 (2018). (https://pubs.acs.org/doi/full/10.1021/acsbiomaterials.8b00403).

Acknowledgement: The author appreciates Drs. H. W. Kroto, J. T. Yates, Z. L. Wang, P. Pulay, C. D. Heyes, and H. C. Tian for fruitful discussions, and all friends and colleagues for supporting this four-year "big data" work.

SUPPLEMENATRY DATA.

I. Extended Data Tables S1–S8.

II. Extended Data Figures S1–S3.

Nanoparticles and atoms geometro-wave potential unified and predicted properties

Z. R. Tian, Chemistry/Biochemistry, and Institute for Nanoscience/Engineering, University of Arkansas, Fayetteville, AR 72701, USA, rtian@uark.edu.

I. Extended Data Tables.

1). Extended Data Table S1**.**

Table S1. Simple-Shape Particles' $\tilde{\nu}_{GW}$ and Point Group of Symmetry

	Shape	Surface-Area (***SA***)	Volume (***V***)	*ṽGW* (= *SA*/*V*)	PntGrpSym
0D		πd^2	$\pi d^3/6$	(6/*d*)*	R_3
1D		$4dL + 2d^2$	$d^2 L$	(4/*d* +2/*L*)** or (4/*d*)** *if* $d << L$	D_{2d}
		$\pi d^2/2 + \pi dL$	$\pi d^2 L/4$	(4/*d* + 2/*L*)** or (4/*d*)** *if* $d << L$	$D_{\infty d}$
2D	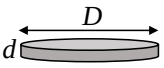	$\pi D^2/2 + d\pi D$	$d\pi D^2/4$	2/*d* + 4/*D*; or 2/*d* *if* $d << D$	$D_{\infty d}$
	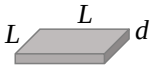	$2(aL + aL + L^2)$	aL^2	2/*d* + 2/*L* + 2/*L*; or 2/*d* *if* $d << L$	D_{4d}
3D		$6d^2$	d^3	(6/*d*)*	O_h
		$2\times3^{1/2}d^2$	$2^{1/2}d^3/3$	$3\times6^{1/2}/d$	O_h
		$1.732d^2$	$0.118d^3$	$14.678/d$	T_d

*The spherical and cubic particles share the same $\tilde{\nu}_{GW}$ formula;
**The two 1D-particles share the same $\tilde{\nu}_{GW}$ formula.

2). Extended Data Table S2**.**

Table S2. Semiconducting 0D-NPs E_g and $\tilde{\nu}_{GW}$

(a). CdS 0D-NP

E_{BG} (eV)	d/6 (nm)	6/d (nm^{-1})
4.78	0.11	9.4
4.22	0.12	8.3
3.89	0.14	7.5
3.72	0.16	6.5
3.32	0.32	3.1
3.05	0.47	2.1
2.68	0.80	1.3

(b). CdSe 0D-NP

E_{BG} (eV)	d/6 (nm)	6/d (nm^{-1})
3.00	0.205	4.9
2.57	0.358	2.8
2.45	0.393	2.6
2.25	0.575	1.7
2.21	0.624	1.6
2.09	0.727	1.4
2.05	0.807	1.2
1.98	0.860	2.2
1.84	1.39	0.72
1.61	1.88	0.53

(c). CdTe 0D-NP

E_{BG} (eV)	d/6 (nm)	6/d (nm^{-1})
2.58	0.4	2.5
2.48	0.47	2.1
2.28	0.57	1.8
2.13	0.62	1.6
2.04	0.68	1.5
1.97	0.71	1.4
1.93	0.82	1.2
1.88	0.87	1.2
1.82	0.95	1.1
1.74	1.3	0.79
1.68	1.4	0.70
1.64	1.6	0.64
1.62	1.8	0.55

3). Extended Data Table S3.

Table S3. Au-0D-NPs melting points and $\tilde{\nu}_{GW}$

d/6 (nm)	6/d (nm^{-1})	T_m (^oK)	d/6 (nm)	6/d (nm^{-1})	T_m (^oK)
0.30	3.330	773	1.05	5.714	1223
0.38	15.79	953	1.13	5.301	1233
0.47	12.77	1043	1.22	4.918	1243
0.55	10.91	1098	1.30	4.615	1251
0.64	9.375	1138	1.38	4.349	1255
0.72	8.333	1163	1.45	4.138	1256
0.80	7.500	1183	1.53	3.922	1262
0.88	6.818	1198	1.62	3.704	1266
0.95	6.316	1208			

4). Extended Data Table S4.

Table S4. Semiconducting CdSe-Nanorod E_g and $\widetilde{\nu}_{GW}$

E_g (eV)	d (nm)	L (nm)	L/d	(SA / V)* (nm^{-1})	E_g (eV)	d (nm)	L (nm)	L/d	(SA / V)* (nm^{-1})
2.20	3.2	11.0	3.4	1.4	2.07	4.3	8.7	2.0	1. 2
2.08	3.3	37.8	12	1.27	2.08	4.3	16.4	3.8	1.1
2.03	3.4	43.1	13	1.23	2.10	4.4	8.6	2.0	1.1
2.11	3.5	28.0	8.0	1.2	1.98	4.4	31.5	7.2	0.97
2.05	3.5	38.5	11	1.2	2.10	4.5	15.3	3.4	1.0
2.17	3.6	11.5	3.2	1.3	2.02	4.6	19.8	4.3	0.97
2.16	3.6	22.1	6.1	1.2	1.97	4.6	19.8	4.3	0.97
2.16	3.7	7.6	2.1	1.3	2.03	4.8	12.4	2.6	0.99
2.19	3.7	9.2	2.5	1.3	2.03	4.8	19.4	4.0	0.94
2.12	3.7	26.1	7.1	1.2	1.93	4.8	40.4	8.4	0.88
2.12	3.7	28.8	7.8	1.2	2.06	4.9	18.4	3.8	0.93
2.12	3.8	8.6	2.3	1.3	2.06	4.9	18.9	3.9	0.92
2.07	3.9	37.2	9.5	1.1	1.99	5.1	12.0	2.4	0.95
2.06	3.9	44.3	11	1.1	2.00	5.2	11.4	2.2	0.94
2.12	4.0	9.7	2.4	1.2	2.00	5.2	22.2	4.3	0.86
2.18	4.0	11.6	2.9	1.2	1.90	5.3	40.8	7.7	0.80
2.02	4.0	41.3	10	1.1	2.00	5.4	18.2	3.4	0.85
2.15	4.1	12.7	3.1	1.1	1.95	5.5	8.5	1.6	0.96
2.13	4.1	13.4	3.3	1.1	1.96	5.5	18.4	3.4	0.84
2.04	4.1	16.9	4.1	1.1	1.97	5.5	23.6	4.3	0.81
2.00	4.1	40.2	9.8	1.0	1.94	6.2	14.0	2.3	0.79
2.06	4.2	16.5	3.9	1.1	1.93	6.4	17.6	2.8	0.74
2.02	4.2	20.2	4.8	1.1					

*** (SA/V)** = (2/L) + (4/d), from the Table 1

5). Extended Data Table S5.

Table S5. Au-0D-NP's λ_{GW}, $\widetilde{\nu}_{GW}$ and λ_{SPR}

d (nm)	λ_{QGD} = d/6 (nm)	$\widetilde{\nu}_{QGD}$ = 6/d (nm^{-1})	λ_{SPR} (nm)
10	1.67	0.60	517.5
15	2.5	0.40	520
20	3.33	0.30	524
30	5	0.20	526
40	6.67	0.15	530
50	8.33	0.12	535
60	10	0.10	540
80	13.33	0.075	553
100	16.67	0.060	572

6). Extended Data Table S6.

Table S6. Main-group atoms polarizability, electronegativity, 1st IP, and $\tilde{\nu}_{GW}$

Atom	Polarizability[3] (10^{-24} cm^3)	EN[3]	1st IP[3] (eV)	d/6[3],[11] (nm)	6/d (nm^{-1})
H	0.667	2.2	13.598	0.0177	56.6
He	0.205		24.587	0.0103	96.8
Li	24.3	0.98	5.391	0.0555	18.0
Be	5.6	1.57	9.322	0.0373	26.8
B	3.03	2.04	8.298	0.029	34.5
C	1.76	2.55	11.26	0.0223	44.8
N	1.1	3.04	14.534	0.0187	53.6
O	0.802	3.44	13.618	0.016	62.5
F	0.557	3.98	17.423	0.01	71.5
Ne	0.39		21.565	0.0127	78.9
Na	24.08	0.93	5.139	0.0633	15.8
Mg	10.6	1.31	7.646	0.0483	20.7
Al	6.8	1.61	5.986	0.0393	25.4
Si	5.38	1.90	8.152	0.0369	27.1
P	3.63	2.19	10.487	0.0327	30.6
S	2.9	2.58	10.36	0.0293	34.1
Cl	2.18	3.16	12.968	0.0263	38.0
Ar	1.62		15.76	0.0236	42.3
K	43.3	0.82	4.341	0.0806	12.4
Ca	22.8	1.00	6.113	0.0645	15.5
Ga	8.12	1.81	5.999	0.0452	22.1
Ge	6.07	2.01	7.899	0.0417	24.0
As	4.31	2.18	9.789	0.038	26.3
Se	3.72	2.55	9.752	0.0342	29.2
Br	3.05	2.96	11.814	0.0313	31.9
Kr	2.48		14.0	0.0293	34.1
Rb	47.3	0.82	4.177	0.0885	11.3
Sr	27.6	0.95	5.695	0.073	13.7
In	10.2	1.78	5.786	0.0518	19.3
Sn	7.7	1.96	7.344	0.0483	20.7
Sb	6.6	2.05	8.608	0.0442	22.6
Te	5.5	2.1	9.01	0.041	24.4
I	5.35	2.66	10.451	0.0342	29.2
Xe	2.6	2.6	12.13	0.036	27.8
Cs	59.6	0.79	3.894	0.099	10.1
Ba	39.7	0.89	5.212	0.084	11.9
Tl	7.6	1.8	6.108	0.0623	15.8
Pb	6.8	1.8	7.417	0.0513	19.5
Bi	7.4	1.9	7.286	0.0476	21.0
Po	6.8	2.0	8.417	0.045	22.2
At	6.0	2.2		0.0424	23.6
Rn	2.2		10.749	0.040	25.0

Note: The superscripts (3) and (11) represent the References #3 and #11.

7). Extended Data Table S7.

Table S7. High-valent monoatomic cations $\tilde{\nu}_{GW}$ and ionization potentials

Cation	d/2 (nm)	6/d (nm^{-1})	IP (eV)
V (II)	0.079	37.97	29.311
V (III)	0.064	46.88	46.71
V (IV)	0.058	51.72	65.28
V (V)	0.054	55.56	128.13
Cr (II)	0.073	41.1	30.96
Cr (III)	0.062	48.39	49.16
Cr (IV)	0.055	54.55	90.635
Cr (VI)	0.044	68.18	160.18
Mn (II)	0.083	36.14	33.668
Mn (III)	0.058	51.72	51.2
Mn (IV)	0.053	56.6	72.4
Mn (V)	0.033	90.91	95.6
Mn (VI)	0.026	115.38	119.203
Mn (VII)	0.025	120	194.5
Mo (III)	0.069	43.48	46.4
Mo (IV)	0.065	46.15	54.49
Mo (V)	0.061	49.18	68.83
Mo (VI)	0.059	50.85	125.67

8). Extended Data Table S8.

Table S8. PbSe 0D-NP

E_g (eV)	6/d (nm^{-1})
0.833	1.18
0.967	1.40
1.077	1.58
1.243	1.88
1.656	2.61

II. Extended Data Figures:

1). Extended Data Fig. S1.

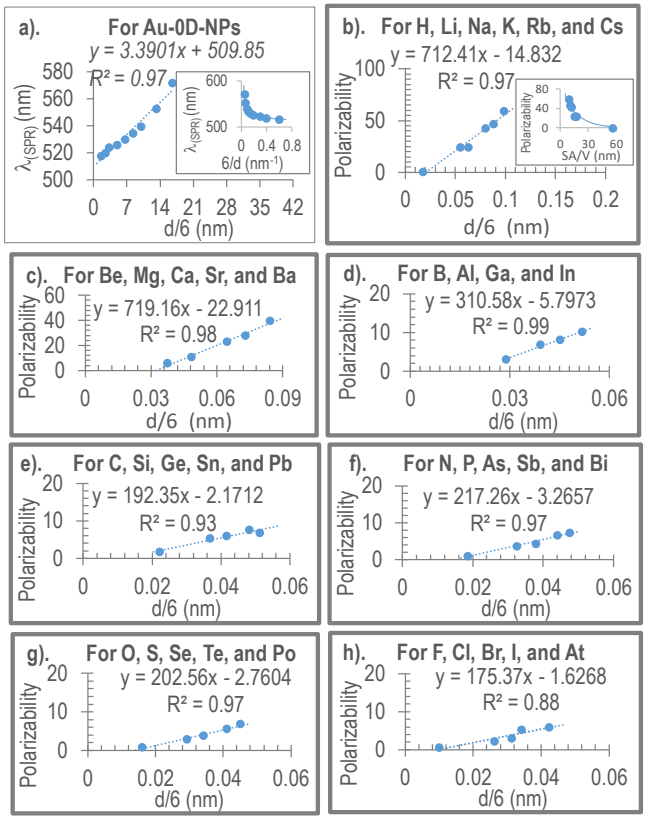

Fig. S1. Linear-fits of λ_{GW}. With Au-0D-NPs' λ_{SPR} (**a**), and main groups atoms' polarizability (**b**)-(**h**). *Note: Tl atom's polarizability far off the linear fit in* ***(d)*** *was omitted*.

2). Extended Data Fig. S2.

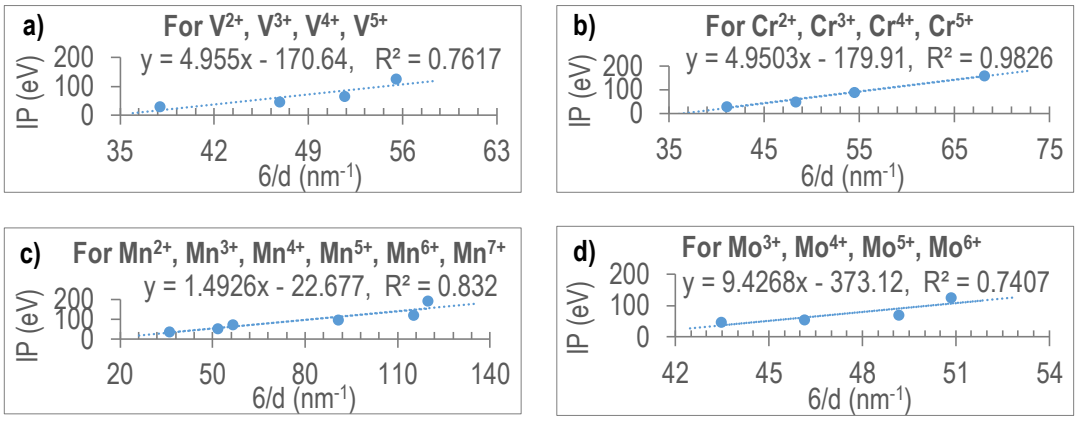

Fig. S2. High-valent cations' IPs in linear correlations with their (6/d) values

3). Extended Data Fig. S3.

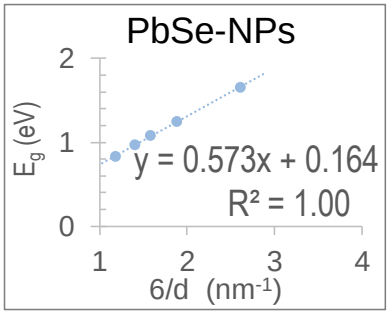

Fig. S3. PbSe-NPs' (6/d) and E_g values in a linear correlation

4). Extended Data Fig. S4.

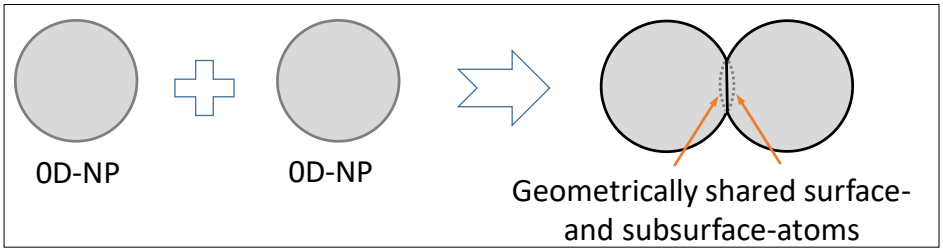

Fig. 3. A model of the chemical bonding between surface-deformed NPs